



Contents lists available at ScienceDirect

International Journal for Parasitology: Parasites and Wildlife

journal homepage: www.elsevier.com/locate/ijppaw

Life cycle truncation in Digenea, a case study of *Neophasis* spp. (Acanthocolpidae)

Georgii Kremnev^{a,*}, Anna Gonchar^{a,b}, Vladimir Krapivin^a, Alexandra Uryadova^a,
Aleksei Mirolubov^{a,b}, Darya Krupenko^a

^a Department of Invertebrate Zoology, Saint Petersburg University, Russia

^b Laboratory of Parasitic Worms and Protists, Zoological Institute, Russian Academy of Sciences, Russia

ARTICLE INFO

Keywords:

Neophasis oculata
Neophasis anarrhichae
Life cycle
Cercariae
Metacercariae
Buccinidae

ABSTRACT

Truncated life cycles may emerge in digeneans if the second intermediate host is eliminated, and the first intermediate host, the mollusc, takes up its role. To understand the causes of this type of life cycle truncation, we analyzed closely related species of the genus *Neophasis* (Acanthocolpidae) with three-host and two-host life cycles. The life cycle of *Neophasis anarrhichae* involves two hosts: wolfish of the genus *Anarrhichas* as the definitive host and the common whelk *Buccinum undatum* as the intermediate host. *Neophasis oculata*, a closely related species with a three-host life cycle, would be a suitable candidate for the comparison, but some previous data on its life cycle seem to be erroneous. In this study, we aimed to redescribe the life cycle of *N. oculata* and to verify the life cycle of *N. anarrhichae* using molecular and morphological methods. Putative life cycle stages of these two species from intermediate hosts were linked with adult worms from definitive hosts using ribosomal molecular data: 18S, ITS1, 5.8S-ITS2, 28S. These markers did not differ within the species and were only slightly different between them. Intra- and interspecific variability was also estimated using mitochondrial COI gene. In the constructed phylogeny *Neophasis* spp. formed a common clade with two other genera of the Acanthocolpidae, *Tormopsolus* and *Pleorchis*. We demonstrated that the first intermediate hosts of *N. oculata* were gastropods *Neptunea despecta* and *B. undatum* (Buccinoidea). Shorthorn sculpins *Myoxocephalus scorpius* were shown to act as the second intermediate and definitive hosts of *N. oculata*. The previous reconstruction of the two-host life cycle of *N. anarrhichae* was reaffirmed. We suggest that life cycle truncation in *N. anarrhichae* was initiated by an acquisition of continuous morphogenesis in the hermaphroditic generation and supported by a strong prey-predator relationship between *A. lupus* and *B. undatum*.

1. Introduction

The diversity of complex life cycles is the most compelling feature of the digenetic trematodes (Digenea). One of the repeated events in the digenean evolution is life cycle truncation, which results in fewer hosts and fewer transmission events involved (Poulin and Cribb, 2002). Secondary dixenous (two-host) life cycles in Digenea may evolve in two major ways. One is progenesis, the transfer of the sexual reproduction into the second intermediate host. The benefits and costs of progenetic development in digeneans and the factors favoring it have been widely discussed and experimentally tested (Lefebvre and Poulin, 2005; Lagrue and Poulin, 2007, 2009; Villa and Lagrue, 2019; etc.). The second way leading to truncated life cycles is the use of the first intermediate host,

the mollusc, as a second intermediate one as well. In this case, the stage of free-swimming cercaria larva is omitted, and the definitive host is infected by consuming the only intermediate host. Such life cycles are known in eleven digenean families (Bartoli et al., 2000; Poulin and Cribb, 2002; Pina et al., 2009). The intriguing question is why most of the digeneans did retain a three-host life cycle even though the use of two hosts and the transmission through the food chain seems to work well enough.

An insight into this question might come from studies of closely related digenean species, some of which have the three-host life cycle and some others, the two-host one. An example can be found in the digenean genus *Neophasis* from the family Acanthocolpidae (Køie, 1973; Bray and Gibson, 1991). Life cycles of acanthocolpids usually involve

* Corresponding author. Department of Invertebrate Zoology, Faculty of Biology, Saint Petersburg University, Universitetskaya emb. 7-9, Saint Petersburg, 199034, Russia.

E-mail addresses: st022767@student.spbu.ru, glistoved69@gmail.com (G. Kremnev).

<https://doi.org/10.1016/j.ijppaw.2021.05.001>

Received 17 March 2021; Received in revised form 1 May 2021; Accepted 1 May 2021

Available online 11 May 2021

2213-2244/© 2021 The Authors. Published by Elsevier Ltd on behalf of Australian Society for Parasitology. This is an open access article under the CC BY-NC-ND

license (<http://creativecommons.org/licenses/by-nc-nd/4.0/>).

three hosts: marine fish as the definitive host, gastropods of the superfamily Buccinoidea as the first intermediate host and fish or bivalves as the second intermediate host (summarized in Kremnev et al., 2020). *Neophasis anarrhichae* (Nicoll, 1909) Bray, 1987 is an exception. It has a two-host life cycle: wolffishes of the genus *Anarrhichas* act as the definitive host and the common whelk *Buccinum undatum* Linnaeus, 1758 is the only intermediate host (Lebour, 1910; Polyansky, 1955; Chubrik, 1966; Køie, 1969). To understand the origin of this condition, we need to examine the three-host life cycles of closely related species, e.g. *Neophasis oculata* (Levinsen, 1881) Miller, 1941. However, it has recently been shown that the life cycle stages from intermediate hosts previously been assigned to *N. oculata* (Chubrik, 1966) actually belong to representatives of the family Brachycladiidae, whose sexual adults are parasites of marine mammals (Kremnev et al., 2020). Thus, the range of intermediate hosts of *N. oculata* is unknown, and the drivers of the life cycle truncation in *N. anarrhichae* remain obscure.

The first aim of the present study was to elucidate the life cycle of *N. oculata*, to verify the life cycle of *N. anarrhichae* and, based on these data, to propose a hypothesis about the origin of the truncated life cycle in the latter species. Another aim was to describe the genetic distance between *N. oculata* and *N. anarrhichae*. Our third objective was to establish the phylogenetic position of the genus *Neophasis* and thus gain some insights on the evolution within the clade Acanthocolpidae + Brachycladiidae.

2. Materials and methods

2.1. Sampling

The definitive hosts of *Neophasis anarrhichae* and *N. oculata*—Atlantic wolffish *Anarrhichas lupus* Linnaeus, 1758 and shorthorn sculpin *Myoxocephalus scorpius* (Linnaeus, 1758)—were caught during summer–autumn of 2019 and 2020 in the White Sea (Keret Archipelago, Kandalaksha Bay, Russia). In total, we dissected 22 individuals of *A. lupus* and 61 individuals of *M. scorpius*. Metacercariae of *N. oculata* were obtained from 12 specimens of *M. scorpius* during the same period of time from three distant localities in the White Sea: Keret Archipelago, Velikaya Salma Strait (Kandalaksha Bay, Russia) and Bolshoy Solovetsky Island (Onega Bay, Russia).

To obtain intramolluscan stages of *Neophasis* spp. we collected and dissected gastropods of the family Buccinidae: *Neptunea despecta* (Linnaeus, 1758), *Buccinum scalariforme* Møller, 1842 and *B. undatum*. The sampling was conducted in 2018–2020 at three localities in the White Sea: Keret Archipelago, Velikaya Salma Strait and Bolshoy Solovetsky Island. Overall, we dissected 73 *N. despecta*, 21 *B. scalariforme* and 1393 *B. undatum*.

2.2. Histology and whole mounts

For whole mounts sexual adults of *N. oculata* and *N. anarrhichae* and metacercariae of *N. oculata* were either flat-fixed in 96% ethanol under the pressure of cover glass or heat-killed and then fixed in 96% ethanol. Intramolluscan stages of both species were fixed in 96% ethanol, or in Shaudin's solution (at 60 °C), or else in saturated solution of mercury (II) chloride with acetic acid (100:1). To visualize the general structure, we used staining with acetic carmine (Sigma Aldrich, Germany) followed by destaining in 0.1 M HCl in 70% ethanol, or staining with toluidine blue (for identification of mucoïd substances). The stained samples were dehydrated in a graded alcohol series and mounted in BioMount medium (Bio Optica, Italy).

Infected snails and metacercariae of *N. oculata* were fixed in Zenker's solution with 40% formaldehyde (10:1) for histological study. After 2 h fixation and 2 h washing in water, the specimens were incubated in 70% ethanol with iodine for 1 h, then transferred into 70% ethanol, dehydrated in a graded alcohol series and embedded in Histomix™ medium (BioVitrum, Russia). Sections were cut at 5 µm and stained in four different ways: with Erlich's hematoxylin and eosin; with Heidenhain's

iron hematoxylin, followed by picric acid destaining; with Mallory's trichrome stain; with Azur II-eosin. The latter stain contains toluidine blue, which is used for visualization of mucoïd substances.

Photographs were made using a compound microscope Leica DM 2500 (Leica Microsystems, Germany) equipped with a Nikon DS Fi3 camera (Nikon, Japan). Measurements of sexual adults and metacercariae were based on heat-killed worms and conducted in Fiji software (Schindelin et al., 2012). All measurements are in micrometers, the range of values is followed by the mean in parentheses.

2.3. Confocal laser scanning microscopy (CLSM)

Staining with antibodies against acetylated α -tubulin and phosphotyrosine (phospho Y) along with the application of tetramethylrhodamine B isothiocyanate (TRITC)-labeled phalloidin and DAPI were used for visualization of various organs including nerves, musculature, excretory and reproductive systems. All the protocols were the same as previously described (Kremnev et al., 2020).

2.4. Scanning electron microscopy

For scanning electron microscopy (SEM) study the specimens were fixed in 2.5% glutaraldehyde in 0.01 M phosphate buffer saline, then rinsed in water, dehydrated in ethanol and acetone, dried in critical point dryer, coated with platinum, and examined with a Quanta 250 SEM at 15 kV.

2.5. Molecular analysis

For molecular analyses, putative and identified life cycle stages of *Neophasis* spp. were fixed in 96% ethanol and stored at 4 °C. Overall, DNA were extracted from 37 isolates (Table 1). For DNA extraction samples were taken from 96% ethanol and dried completely, incubated in 200 µL of 5% Chelex® 100 resin (Bio-Rad, USA) solution with 0.2 mg/mL of proteinase K at 56 °C for 4 h, then kept for 8 min at 90 °C and centrifuged at 16,000 g for 10 min. The supernatant containing DNA was then transferred to a new tube and stored at –20 °C.

Several primers were used to amplify fragments of ribosomal operon and the mitochondrial COI gene (Table 2). Amplifications were performed in 20 µL reaction mixtures containing 13 µL of Milli-Q® water (Merck Millipore Co., Germany), 4 µL of ScreenMix-HS reaction mix (Evrogen, Russia), 0.5 µL of both F and R primers, and 2 µL of DNA template. PCR products were visualized on a 1% agarose gel stained with ethidium bromide (Helicon, Moscow), and sequenced with PCR primers on an ABI Prism 3500xl genetic analyzer (Applied Biosystems, MA, USA). Sequence data were processed and analyzed using Geneious® 2021.0.2 (<https://www.geneious.com>). We used the Geneious plugin Repeat Finder 1.0 (Biomatters Ltd.) to detect repeats in the sequences. When the repeat regions hindered the alignment, they were excluded. To estimate the boundaries between all the elements of the ribosomal operon, we used the annotated sequence (KR703279) of *Brachycladium goliath* (van Beneden, 1858) Fraija-Fernández, Aznar, Raga, Gibson & Fernández, 2014, Brachycladiidae (Briscoe et al., 2016). Annotated mitochondrial genome (KR703278) of the same digenean species was used to determine the position of amplified COI fragments. Mean pairwise genetic distance within and between species (as a number of base differences per site) and standard error were calculated in MEGA 7 under the Maximum Composite Likelihood model (Kumar et al., 2016). To assess the quality of the protein-coding nucleotide sequences, we translated them (code 21) to make sure that stop codons were absent and the resulting amino acid sequence corresponded to the expected product. Translated sequences were also used to identify synonymous and non-synonymous substitutions, and to predict the functional effect of the latter in Provean (Choi and Chan, 2015).

Relevant data from GenBank were included into the SSU and LSU alignments (Supplementary Table S1). The best model of nucleotide

Table 1

Isolates of putative and identified Acanthocolpidae from the White Sea, their origin and GenBank accession numbers.

Isolate number	Stage	Host	Locality	ID	SSU	LSU	ITS1	5.8S-ITS2	COI
<i>Neophasis oculata</i>									
1	Sexual adult	<i>Myoxocephalus scorpius</i>	Keret Archipelago (Kandalaksha Bay, Russia)	13.48s	–	MW730773	MW750246	MW750294	MW731655
2	Sexual adult	<i>Myoxocephalus scorpius</i>	Keret Archipelago (Kandalaksha Bay, Russia)	86.51s.1	MW730771	MW730774	MW750247	MW750295	MW731656
3	Sexual adult	<i>Myoxocephalus scorpius</i>	Keret Archipelago (Kandalaksha Bay, Russia)	86.51s.2	–	–	MW750248	MW750296	MW731657
Putative <i>N. oculata</i>									
4	Metacercaria	<i>Myoxocephalus scorpius</i>	Keret Archipelago (Kandalaksha Bay, Russia)	56.48s	–	MW730775	–	MW750296	MW731658
5	Metacercaria	<i>Myoxocephalus scorpius</i>	Bolshoy Solovetsky Island (Onega Bay, Russia)	386.51s	–	–	MW750249	MW750298	MW731659
6	Metacercaria	<i>Myoxocephalus scorpius</i>	Velikaya Salma Strait (Kandalaksha Bay, Russia)	484.51s	–	–	MW750250	MW750299	MW731660
7	Metacercaria	<i>Myoxocephalus scorpius</i>	Keret Archipelago (Kandalaksha Bay, Russia)	542.51s	–	–	MW750251	MW750300	MW731661
8	Daughter redia containing embryos and cercariae	<i>Buccinum undatum</i>	Keret Archipelago (Kandalaksha Bay, Russia)	15.45s	–	MW730776	MW750252	MW750301	MW731662
9	Daughter redia containing embryos and cercariae	<i>Buccinum undatum</i>	Keret Archipelago (Kandalaksha Bay, Russia)	15.47s	–	–	MW750253	MW750302	MW731663
10	Daughter redia containing embryos and cercariae	<i>Buccinum undatum</i>	Keret Archipelago (Kandalaksha Bay, Russia)	22.47s	–	MW730777	–	MW750303	MW731664
11	Daughter redia containing embryos and cercariae	<i>Buccinum undatum</i>	Keret Archipelago (Kandalaksha Bay, Russia)	291.48s	–	MW730778	–	MW750304	MW731665
12	Daughter redia containing embryos and cercariae	<i>Buccinum undatum</i>	Keret Archipelago (Kandalaksha Bay, Russia)	485.51s	–	MW730779	MW750254	MW750305	MW731666
13	Daughter redia containing embryos and cercariae	<i>Neptunea despecta</i>	Keret Archipelago (Kandalaksha Bay, Russia)	172.48s	–	MW730780	MW750255	MW750306	–
14	Daughter redia containing embryos and cercariae	<i>Neptunea despecta</i>	Keret Archipelago (Kandalaksha Bay, Russia)	327.48s	–	MW730781	MW750256	MW750307	MW731667
15	Daughter redia containing embryos and cercariae	<i>Neptunea despecta</i>	Keret Archipelago (Kandalaksha Bay, Russia)	432.51s	–	MW730782	MW750257	MW750308	MW731668
16	Daughter redia containing embryos and cercariae	<i>Neptunea despecta</i>	Keret Archipelago (Kandalaksha Bay, Russia)	534.51s	–	–	MW750258	MW750309	MW731669
17	Daughter redia containing embryos and cercariae	<i>Neptunea despecta</i>	Velikaya Salma Strait (Kandalaksha Bay, Russia)	349.48s	–	MW730783	MW750259	MW750310	–
18	Daughter redia containing embryos and cercariae	<i>Neptunea despecta</i>	Velikaya Salma Strait (Kandalaksha Bay, Russia)	352.48s	–	–	MW750260	MW750311	MW731670
<i>Neophasis anarrhichae</i>									
19	Sexual adult	<i>Anarrhichas lupus</i>	Keret Archipelago (Kandalaksha Bay, Russia)	149.48s	–	MW730784	MW750261	MW750312	–
20	Sexual adult	<i>Anarrhichas lupus</i>	Keret Archipelago (Kandalaksha Bay, Russia)	504.51s.1	MW730772	MW730785	MW750262	MW750313	MW731671
21	Sexual adult	<i>Anarrhichas lupus</i>	Keret Archipelago (Kandalaksha Bay, Russia)	504.51s.2	–	MW730786	MW750263	MW750314	MW731672
22	Sexual adult	<i>Anarrhichas lupus</i>	Keret Archipelago (Kandalaksha Bay, Russia)	323.51s.1	–	MW730787	MW750264	MW750315	MW731673
23	Sexual adult	<i>Anarrhichas lupus</i>	Keret Archipelago (Kandalaksha Bay, Russia)	323.51s.2	–	MW730788	MW750265	MW750316	MW731674
24	Sexual adult	<i>Anarrhichas lupus</i>		146.51s.1	–	MW730789	MW750266	MW750317	MW731675

(continued on next page)

Table 1 (continued)

Isolate number	Stage	Host	Locality	ID	SSU	LSU	ITS1	5.8S-ITS2	COI
25	Sexual adult	<i>Anarhichas lupus</i>	Keret Archipelago (Kandalaksha Bay, Russia)	146.51s.2	–	–	MW750267	MW750318	MW731676
Putative <i>N. anarrhichae</i>									
26	Daughter rediae containing embryos and cercariae	<i>Buccinum undatum</i>	Keret Archipelago (Kandalaksha Bay, Russia)	319.51s	–	–	MW750268	MW750319	MW731677
27	Daughter rediae containing cercariae	<i>Buccinum undatum</i>	Keret Archipelago (Kandalaksha Bay, Russia)	259.48s	–	MW730790	MW750269	MW750320	MW731678
28	Daughter rediae containing cercariae	<i>Buccinum undatum</i>	Keret Archipelago (Kandalaksha Bay, Russia)	47.51s	–	–	MW750270	MW750321	MW731679
29	Daughter rediae containing cercariae and metacercariae	<i>Buccinum undatum</i>	Keret Archipelago (Kandalaksha Bay, Russia)	240.48s	–	–	MW750271	MW750322	MW731680
30	Daughter rediae containing cercariae and metacercariae	<i>Buccinum undatum</i>	Keret Archipelago (Kandalaksha Bay, Russia)	279.51s	–	–	MW750272	MW750323	MW731681
31	Daughter rediae containing metacercariae	<i>Buccinum undatum</i>	Keret Archipelago (Kandalaksha Bay, Russia)	491.51s	–	–	MW750273	MW750324	MW731682
32	Daughter rediae containing progenetic metacercariae	<i>Buccinum undatum</i>	Keret Archipelago (Kandalaksha Bay, Russia)	127.48s	–	MW730791	MW750274	MW750325	MW731683
33	Daughter rediae containing progenetic metacercariae	<i>Buccinum undatum</i>	Keret Archipelago (Kandalaksha Bay, Russia)	500.51s	–	–	MW750275	MW750326	MW731684
Putative Acanthocolpidae									
34	Mother sporocyst	<i>Buccinum undatum</i>	Keret Archipelago (Kandalaksha Bay, Russia)	444.51s	–	–	MW750276	MW750327	MW731685
35	Mother redia	<i>Buccinum undatum</i>	Keret Archipelago (Kandalaksha Bay, Russia)	445.51s	–	–	MW750277	MW750328	MW731686
36	Mother redia	<i>Buccinum undatum</i>	Keret Archipelago (Kandalaksha Bay, Russia)	282.51s	–	–	MW750278	MW750329	MW731687
37	Mother redia	<i>Buccinum undatum</i>	Keret Archipelago (Kandalaksha Bay, Russia)	292.51s	–	–	MW750279	MW750330	MW731688

Table 2

PCR primers and thermocycling conditions; in all reactions initial denaturation was at 95 °C for 5 min and final extension was at 72 °C for 10 min.

Product	Primer	Sequence (5'-3'), forward (F) and reverse (R)	Thermocycling profile	Reference
18S rDNA	18S1A	F, GCGCATCGAAAAGATTAAGCCATGCA	94 °C — 1m	Hernández-Mena et al. (2017) (primers and conditions)
	32	R, CGAAGTCCTATTCCATTATTC	52 °C — 1m	
	652	F, GCAGCCGCGGTAATTCAGCTC	72 °C — 1m	
28S rDNA	28	R, AGCGACGGGCGGTGTGT	× 35	Tkach et al. (1999) (primers and conditions) Olson et al. (2003) (primers and conditions)
	dig12	F, AAGCATATCACTAAGCGG	95 °C–30s	
	1500R	R, GCTATCCTGAGGGAAACTTCG	54 °C–30s 72 °C — 2m × 40	
ITS1	BD1	F, GTCGTAACAAGGTTTCCGTA	95 °C–30s	Luton et al. (1992) (primers and conditions)
	4S	R, TCTAGATGCGTTCGAARTGTCGATG	55 °C–30s 72 °C — 1m × 35	
5.8S-ITS2	3S	F, GTACCGGTGATCAGCTGGCTAGTG	94 °C–30s	Morgan and Blair (1995) (primers)
	ITS2.2	R, CCTGTTAGTTTCTTTCTCCCGC	55 °C–30s 72 °C — 1m × 30	
COI	JB3	F, TTTTTGGGCATCCTGAGGTTTAT	95 °C–30s	Bowles et al. (1993) (primers and conditions)
	JB4.5	R, TAAAGAAAGAACATAATGAAATG	50 °C–30s 72 °C — 1m × 35	
COI	JB3	F, TTTTTGGGCATCCTGAGGTTTAT	95 °C–30s	Leung et al. (2009) (primers and conditions)
	trem.cox1.rml	R, AATCATGATGCAAAAGGTA	48 °C–40s 72 °C — 1m × 40	

substitution was estimated as GTR + G + I using jModelTest (Darriba et al., 2012) at the CIPRES Science Gateway (<https://www.phylo.org>). The maximum likelihood (ML) analysis was conducted using RAxML (Stamatakis, 2014) at the CIPRES Science Gateway. The stability of clades was assessed using non-parametric bootstrapping with 1000 pseudoreplicates. The Bayesian analysis was conducted using MrBayes v.3.2.6 (Ronquist et al., 2012) with 10,000,000 generations.

3. Results

3.1. Morphological identification of the *Neophasis* spp. life cycle stages

We found sexual adults of the Acanthocolpidae, which could easily be recognized as *Neophasis oculata* and *N. anarrichae* in *Myoxocephalus scorpius* and *Anarrichas lupus*, respectively. We identified the acanthocolpid metacercariae from *M. scorpius* as *N. oculata* since this is the only known acanthocolpid species in the White Sea which encysts in fish (Shulman and Shulman-Albova, 1953). Many cases of acanthocolpid infection were found in *Buccinum undatum* and several, in *Neptunea despecta*; no specimens of *B. scalariforme* were infected. Intramolluscan stages of Acanthocolpidae from *B. undatum* predominantly corresponded to the previously described life cycle stages of *N. anarrichae*

(Lebour, 1910; Chubrik, 1966; Kõie, 1969). However, in several infected specimens of *B. undatum* and all infected specimens of *N. despecta* we found acanthocolpid cercariae with much more prominent eyespots. We suggested that these might belong to *N. oculata*. Finally, we discovered a mother sporocyst and mother rediae in several *B. undatum* specimens and supposed that they might belong to the Acanthocolpidae.

3.2. Molecular genetic data and life cycles elucidation

To check our morphological identification and link life cycle stages from intermediate hosts and sexual adults from definitive hosts, we extracted DNA from 37 isolates (Table 1). We sequenced fragments of the ribosomal operon and partial mitochondrial COI gene from this material and submitted these data to GenBank (accession numbers are given in Table 1).

For all the 37 samples, we sequenced a 493 b.p. fragment containing partial 5.8S rDNA, complete ITS2 and the start of the 28S rDNA. The only detected variation was in position 99 (5.8S rDNA). It clearly differentiated the sexual adults of *N. oculata* (A) and *N. anarrichae* (T). A difference between these species was also found in the 18S rDNA sequences. They were obtained for one sexual adult of each species, *N. oculata* (1707 b.p.) and *N. anarrichae* (1636 b.p.), and differed by two

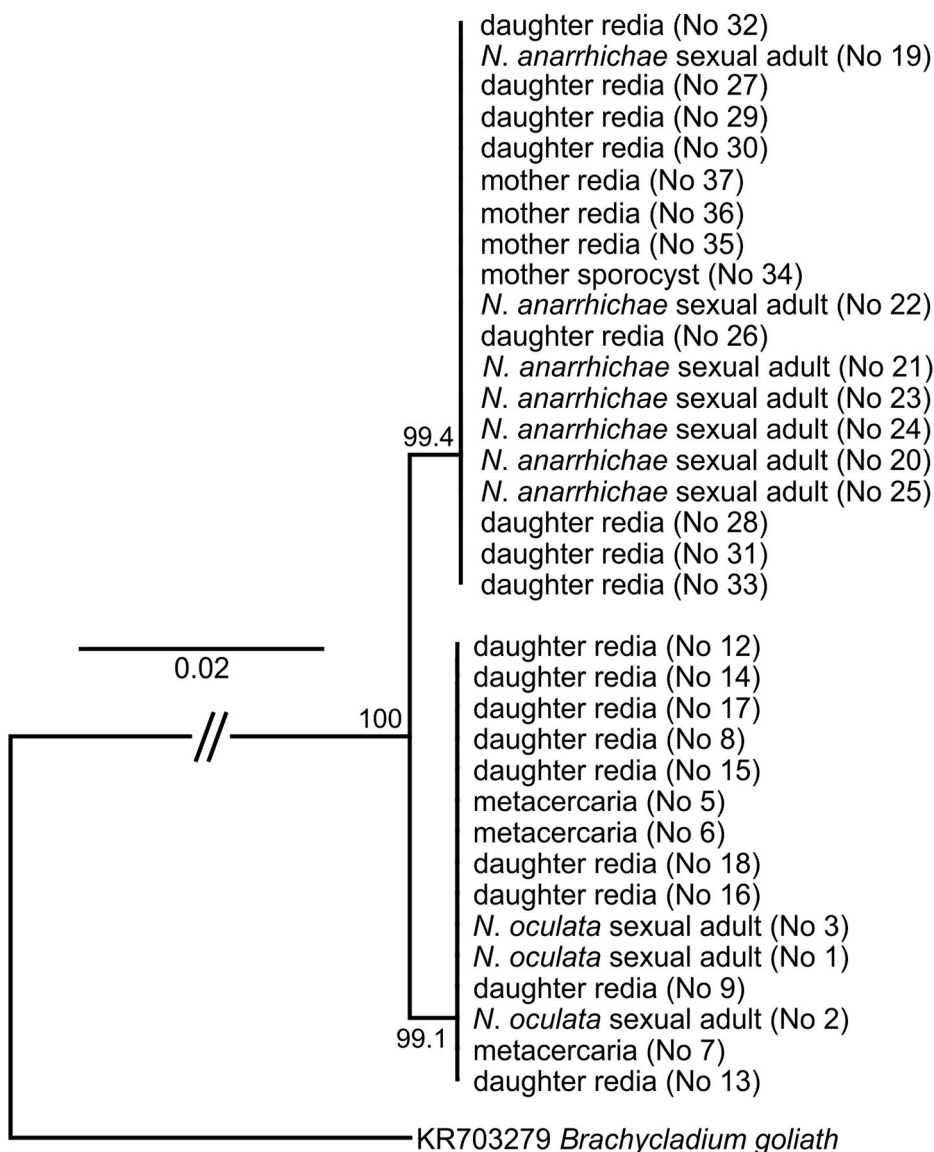


Fig. 1. Consensus (99 threshold) neighbour-joining tree based on the concatenated ITS1 and ITS2 860-b.p. fragment, built with Tamura-Nei genetic distance method and 1000 bootstrap resamples; support values are printed at nodes. Repeat regions of the ITS1 were excluded from the alignment. Scale bar shows substitutions per site. The ingroup includes identified and putative life cycle stages of *Neophasis oculata* and *N. anarrichae*, the numbers of isolates are as listed in Table 1. *Brachycladium goliath* serves as an outgroup.

nucleotide substitutions. *Neophasis oculata* and *N. anarrichae* also diverged in the ITS1 region. Out of the 34 ITS1 sequences, 15 were 925 b.p. long and 19 were 831 b.p. long. Their 5'-part contained 47 b.p.-long repeats. The difference in the product length by 94 b.p. was due to the repeat number variation: nine in *N. oculata* and seven in *N. anarrichae*. In addition, these species differed by eight nucleotide substitutions in the ITS1, five within the repeat region and three outside it.

All the genetic differences in the ribosomal operon mentioned above were consistent and made it possible to outline two groups of samples. The first one comprised all the sexual adults of *N. anarrichae* (7), putative daughter rediae of *N. anarrichae* (8), a mother sporocyst (1) and mother rediae (3). The second group comprised all the sexual adults of *N. oculata* (3), putative metacercariae of *N. oculata* (4) and putative daughter rediae of *N. oculata* (11). No genetic difference was detected within each group. One more ribosomal marker, the partial 28S rDNA (1263–1270 b.p. long), was sequenced for 19 isolates, but did not show any variation. Overall, we outlined subtle but consistent genetic distinctions in rDNA between *N. oculata* and *N. anarrichae* and linked putative life cycle stages from the intermediate hosts and sexual adults from the definitive hosts of both species (Fig. 1).

Aiming to amplify the mitochondrial COI gene with JB3/JB4.5 primers, we obtained eighteen 387–406 b.p. long sequences of identified *N. anarrichae*. These sequences, which appeared to be identical, had a frameshift inside caused by two deletions and thus could not be translated into a functional protein. These were interpreted as a possible nuclear copy of a mitochondrial gene (numt). We submitted one such sequence to GenBank under accession number MW740397 and did not analyze it further. The primer pair JB3/trem.cox1.rnr1 yielded sequences that were 770 b.p. long after trimming in both species, contained no stop codons and were translated into a COI protein. These sequences were used in the alignments.

In *N. oculata*, the alignment of 16 COI sequences had eight polymorphic sites, four of which were singletons. Mean intraspecific pairwise distance was 0.0030 ± 0.0013 substitutions per site. Seven nucleotide substitutions were synonymous; two amino acid substitutions in positions 217 (Ile→Thr) and 248 (Phe→Leu) were predicted to be neutral. In *N. anarrichae*, the alignment of 18 COI sequences had 12 polymorphic sites, three of which were singletons. Mean intraspecific pairwise distance was 0.0040 ± 0.0016 substitutions per site. Eight nucleotide substitutions were synonymous; four amino acid substitutions in positions 107 (Met→Thr), 172 (Ile→Val), 218 (Val→Ala), 248 (Leu→Phe) were predicted to be neutral. The mean interspecific divergence was 0.1573 ± 0.0887 substitutions per site.

3.3. Infection data and morphological descriptions

3.3.1. Intramolluscan stages of *Neophasis oculata* (Fig. 2)

Locality: White Sea; Keret Archipelago, Velikaya Salma Strait (Kandalaksha Bay).

Hosts: *Buccinum undatum*, *Neptunea despecta*.

Sites: Reproductive and digestive gland.

Prevalence: 0.4% (5 of 1376) *B. undatum* in Keret Archipelago; 7% (5 of 68) *N. despecta* in Keret Archipelago; 66% (2 of 3) *N. despecta* in Velikaya Salma Strait.

Vouchers: Isogenophores (NO006–NO011) corresponding to isolates No 9, 10 and 13 deposited in the collection of the Department of Invertebrate Zoology of Saint Petersburg University.

Description:

Daughter rediae (Fig. 2A).

[Measurements based on 20 specimens fixed with saturated solution of mercury (II) chloride with acetic acid: 10 specimens from *B. undatum* and 10 specimens from *N. despecta*.]

Rediae elongated, sausage-shaped, 828–1964 (1345) × 133–251 (181). Posterior end usually pointed. Mouth terminal, pharynx small, oval, 35–51 (44) × 18–48 (35). Cecum oval, short, 33–111 (65) × 24–46 (32). Brood cavity occupying almost all inner space of rediae, containing

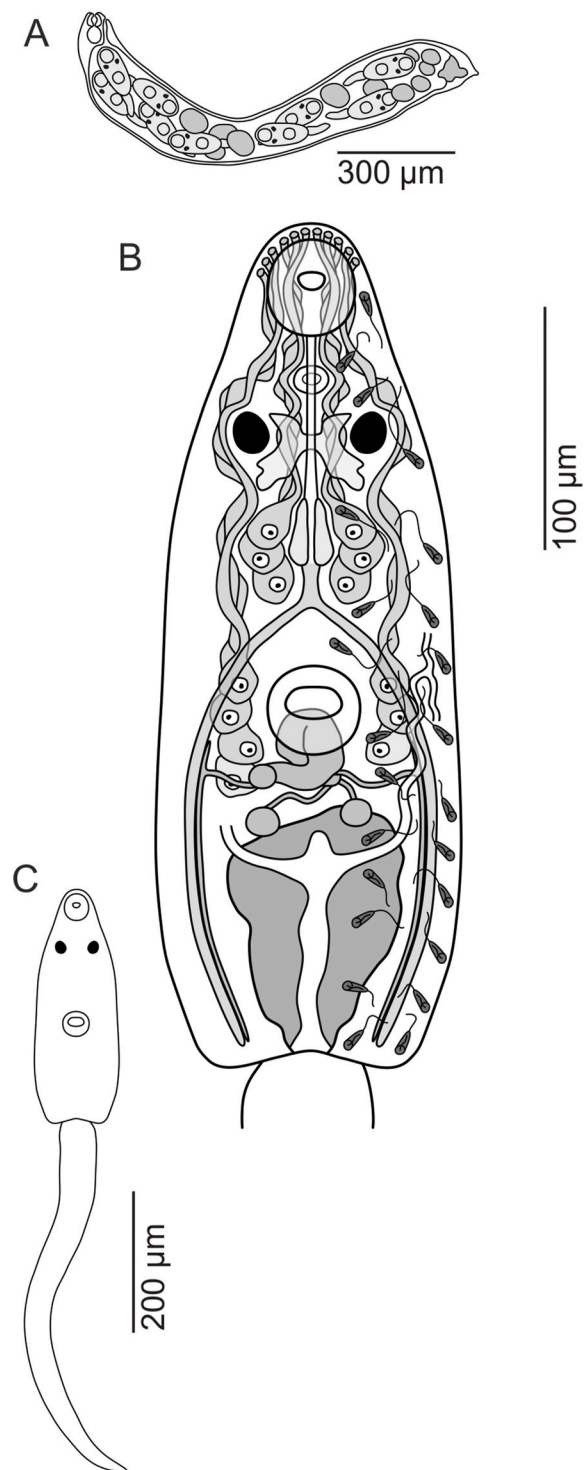


Fig. 2. *Neophasis oculata* intramolluscan stages: daughter redia (A), infective cercaria body structure (B) and general view (C).

cercarial embryos at different stages of development. Birth pore with distinct birth canal posterior to pharynx. Germinal mass at posterior body end, embedded in parenchyma.

Cercariae (Fig. 2B and C).

[Measurements based on 20 specimens fixed with saturated solution of mercury (II) chloride with acetic acid.]

Distome larvae with pair of pigmented eyespots and simple tail (Fig. 2C). Body 245–504 (356) long, 90–139 (116) wide, bottle-shaped, with narrowed anterior and dilated posterior ends (Fig. 2B; 3A, F).

Spines small, simple; size and density decreasing towards posterior end (Fig. 3F). Tail simple, 260–826 (524) long, 33–52 (46) wide at base (Fig. 2C; 3A). Oral sucker subterminal, oval, 35–58 (46) × 34–48 (40). Ventral sucker spherical, 33–50 (42) × 35–47 (40), near center of body, slightly closer to posterior end (Fig. 2B; 3A, F). Sucker-ratio 1:0.67–1.23 (0.93). Prepharynx long (Fig. 2B). Pharynx pyriform to oval (Figs. 2B and 3A, B, H, I), 21–26 (24) × 11–18 (14). Oesophagus primordium short (Fig. 2B; 3A, H). Ceca primordia as rows of cells, extending to posterior body end, lateral to excretory vesicle (Fig. 2B; 3A, H). Cerebral ganglion dorsal to prepharynx (Fig. 2B; 3A, B, G). Two pigmented eyespots, large, oval, lateral to oesophagus (Fig. 2B; 3A-E, H, I). Phospho Y positive structure (unpaired unpigmented eyespot) anteromedial to pigmented eyespots (Fig. 2B; 3I); also staining with TRITC-labeled phalloidin (Fig. 3I). Thirteen small unicellular penetration glands in two groups (Fig. 2B; 3A). Anterior group of six glands in forebody, lateral to pharynx (Fig. 2B; 3A); ducts running medially to pigmented eyespots towards anterior body end (Fig. 2B; 3B). Posterior group of seven glands lateral and posterior to ventral sucker (Fig. 2B; 3A); only five ducts present, running lateral to anterior penetration glands and pigmented eyespots towards anterior body end (Figs. 2B and 3B). Each duct opening through individual pore near anterior edge of oral sucker, 11 pores in total (Fig. 2B). Cystogenous glands not detected. Excretory vesicle in hindbody, I-shaped, voluminous, slightly asymmetrical

(Fig. 2B; 3A, C); sometimes appearing Y-shaped, due to dilated proximal parts of main collecting ducts. Excretory vesicle wall thick, staining slightly with eosin (Fig. 3C). Excretory system of “Mesostoma” type (Fig. 2B). Main collecting ducts dividing into anterior and posterior parts near anterior edge of ventral sucker. Excretory formula $2[(4 + 4 + 4) + (4 + 4 + 4)] = 48$. Caudal excretory duct present in underdeveloped cercariae and absent in infective cercariae (Fig. 2B; 3H). Small testes primordia in hindbody, slightly oblique; posterior testis slightly larger than anterior one (Fig. 2B). *Vasa efferentia* visible (Fig. 2B). Cirrus-sac primordium as C-shaped group of cells (Fig. 2B). Primordium of female reproductive system crooked, compact (including metraterm, uterus, ootype, Laurer’s canal, oviduct and ovary); from its dorsal part vitellarium primordium passing as two strands of cells laterally, then dividing into short anterior and long posterior part (Fig. 2B).

Developing cercariae and mucoïd structures (Fig. 3A, D, E).

Cercariae leave rediae underdeveloped, and morphogenesis is completed in the digestive gland of the host. Development of pigmented eyespots begins soon after formation of the tail bud (Fig. 2A). Mucoïd glands as described in Xiphidiata and Opisthorchiata are absent. Mucoïd substances were found in cytons at the dorsal side of the body, and in the tail of cercaria embryos (Fig. 3D and E). Development of mucoïd cytons begins before the larvae leave the rediae (Fig. 3E). During the final stages of cercarial development outside rediae, the mucoïd substance is

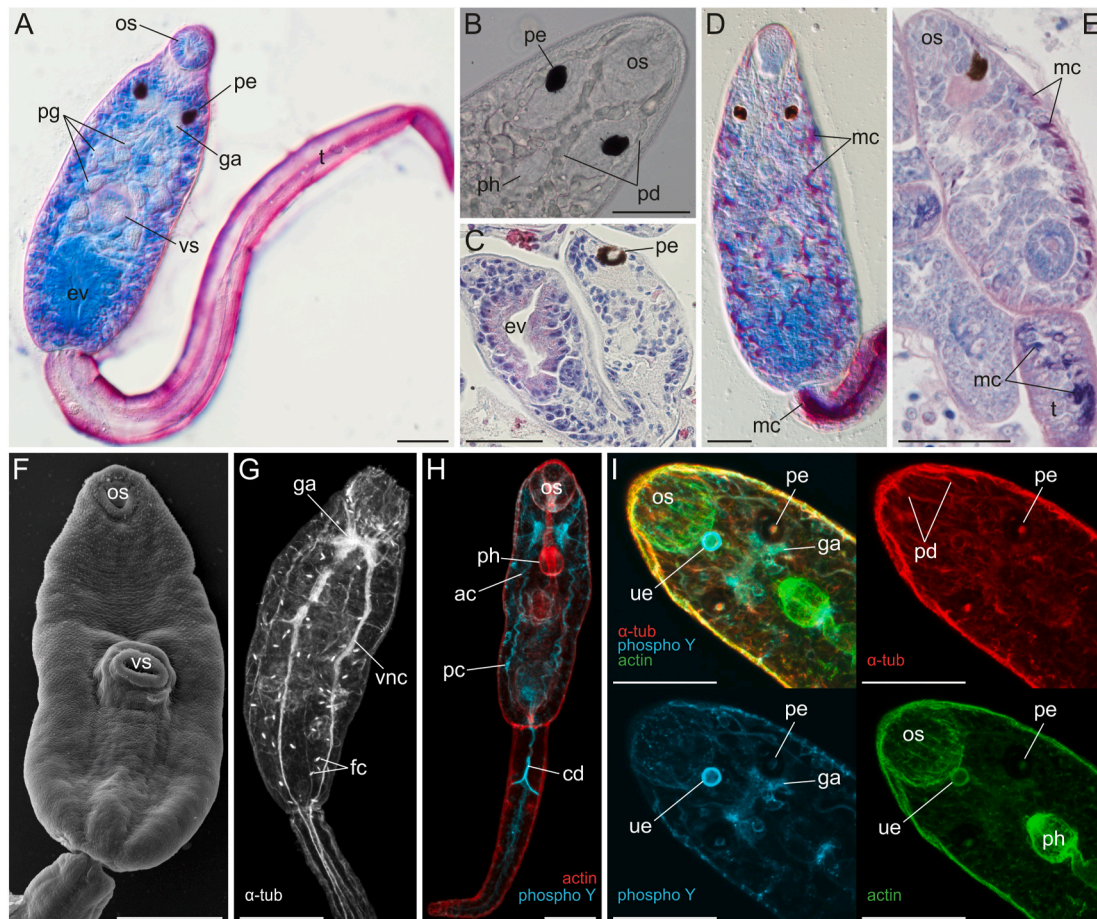


Fig. 3. *Neophasis oculata* cercariae. (A) Infective cercaria, general structure and mucoïd in the tegument (toluidine blue), differential interference contrast (DIC). (B) Ducts of the penetration glands in live cercaria. (C) Sagittal histological section of infective cercaria, Erlich's hematoxylin-eosin. (D-E) Mucoïd in underdeveloped cercariae (toluidine blue, whole mount, DIC (D) and Azur II-eosin, histological section (E)). (F) SEM, ventral view. (G-I) CLSM, TRITC-phalloidin, acetylated α -tubulin and phospho Y antibody staining. (G) Infective cercaria, flame cells and nerves. (H-I) Underdeveloped cercariae, excretory ducts (H) and eyespots (I). Scale bars - 50 μ m. Abbreviations: ac - anterior collecting duct; cd - caudal excretory duct; ev - excretory vesicle; fc - flame cells; ga - cerebral ganglion; mc - mucoïd cytons; os - oral sucker; pc - posterior collecting duct; pe - pigmented eyespots; pg - penetration glands; pd - penetration gland ducts; ph - pharynx; t - tail; ue - unpigmented eyespot; vnc - ventral nerve chords; vs - ventral sucker. (For interpretation of the references to colour in this figure legend, the reader is referred to the Web version of this article.)

Table 3
Dimensions and taxonomic characters of the White Sea *Neophasis* spp.

	<i>Neophasis oculata</i> (sexual adults)	<i>Neophasis oculata</i> (metacercariae, n = 10)	<i>Neophasis anarrhichae</i> (sexual adults)
Length	795-1135 (922) (n = 11)	631-828 (728)	431-653 (558) (n = 16)
Width	233-326 (272) (n = 11)	175-232 (204)	153-216 (188) (n = 16)
Forebody, length	283-444 (373) (n = 11)	218-332 (284)	149-257 (201) (n = 16)
Forebody, % of body length	26-45 (41) (n = 11)	32-44 (39)	32-39 (36) (n = 16)
Oral sucker	83-99 × 85-97 (91 × 91) (n = 11)	57-77 × 62-84 (66 × 73)	75-94 × 80-103 (83 × 89) (n = 16)
Ventral sucker	87-110 × 83-113 (98 × 97) (n = 11)	63-88 × 55-82 (75 × 69)	73-93 × 73-106 (83 × 94) (n = 16)
Sucker-ratio	1:1.0-1.24 (1.09) (n = 11)	1:1.09-1.24 (1.15)	1:0.87-1.10 (0.99) (n = 16)
Prepharynx	61-207 (125) (n = 10)	59-146 (108)	33-60 (43) (n = 10)
Pharynx	61-87 × 56-79 (78 × 70) (n = 10)	46-59 × 52-73 (51 × 62)	64-72 × 51-65 (67 × 60) (n = 10)
Oesophagus	44-82 (56) (n = 10)	37-56 (49)	15-33 (26) (n = 10)
IB-VS	19-64 (37) (n = 10)	15-39 (25)	0-24 (10) (n = 10)
Vit-VS	56-118 (85) (n = 10)	–	18-82 (49) (n = 10)
VS-Ovary	0-86 (50) (n = 10)	21-70 (41)	22-70 (42) (n = 10)
Ovary	62-86 × 48-77 (74 × 66) (n = 10)	34-54 × 30-48 (41 × 38)	59-74 × 47-62 (66 × 55) (n = 10)
Testis, anterior	102-150 × 59-147 (128 × 107) (n = 11)	66-107 × 48-96 (84 × 77)	69-104 × 55-84 (85 × 68) (n = 14)
Testis, posterior	103-158 × 63-142 (136 × 117) (n = 11)	69-130 × 53-106 (98 × 85)	80-123 × 50-82 (96 × 65) (n = 14)
Testes overlap, %	25-97 (53) (n = 11)	11-79 (43)	0-94 (52) (n = 16)
Lateral testes overlap, %	0-65 (26) (n = 11)	0-18 (4)	0-37 (22) (n = 16)
PTR	111-174 (143) (n = 11)	113-163 (137)	58-93 (76) (n = 16)
PTR, % of body length	13-18 (16) (n = 11)	17-22 (19)	10-18 (14) (n = 16)
C-PE	25-50 (40) (n = 10)	20-49 (37)	30-77 (49) (n = 10)
Eggs, number	1-5 (3) (n = 10)	–	2-6 (4) (n = 10)
Egg-size	76-117 × 36-56 (96 × 43) (n = 27)	–	64-109 × 32-59 (91 × 43) (n = 27)

IB-VS. Distance from intestinal bifurcation to anterior margin of ventral sucker.
Vit-VS. Distance from anterior-most extent of vitelline fields to anterior margin of ventral sucker

VS-Ovary. Distance from posterior margin of ventral sucker to anterior margin of ovary.

PTR. Length of post-testicular region.

C-PE. Distance from posterior-most extent of the intestinal caeca to posterior extremity of worm.

pyloric caeca. In heavily infected fish, the worms were also found in the other regions of the digestive tract such as the stomach, the midgut and the hindgut.

3.3.4. Intramolluscan stages of *Neophasis anarrhichae* (Fig. 6, 7A-I)

Locality: White Sea; Keret Archipelago (Kandalaksha Bay).

Host: *Buccinum undatum*.

Sites: Reproductive and digestive gland (mother and daughter rediae); kidney (mother sporocyst and mother rediae). In heavily infected whelks, daughter rediae were also located in kidney, gill and mantle.

Prevalence: 5% (69 of 1376).

Vouchers: Hologenophore VG5.3 (mother sporocyst) and isogenophores (NA004-NA010) corresponding to isolates No 29, 32, 34, 35 and 36 deposited in the collection of the Department of Invertebrate Zoology of Saint Petersburg University.

Description:

Mother sporocyst (Fig. 6A).

In single found specimen body elongated, 994 × 211, anterior end wide, posterior end pointed. Brood cavity occupying almost all inner space, containing nine embryos of mother rediae, with one embryo much more advanced than others. Birth pore not identified with certainty but probably located at anterior end. Germinal mass at posterior end, embedded in parenchyma.

Mother rediae (Fig. 6B).

[Measurements based on ten specimens from kidney fixed with 96% ethanol.]

Rediae elongated, 272–836 (595) × 61–146 (104), capable of slight contraction, with pointed posterior end. Mouth terminal, pharynx small, oval, 34–69 (48) × 25–56 (42). Cecum oval, 27–92 (66) × 22–61 (41). Brood cavity occupying almost all inner space of rediae, containing embryos of daughter rediae at different stages of development. Birth pore with distinct birth canal posterior to pharynx. Germinal mass at posterior body end, embedded in parenchyma. In younger rediae cecum occupying nearly one third of body length; brood cavity indistinct, without embryos.

Daughter rediae, cercariae and metacercariae (Fig. 7A–I).

These life cycle stages of *Neophasis anarrhichae* have been described elsewhere (Lebour, 1910; Chubrik, 1966; Kōie, 1969, 1971). Nevertheless, we would like to specify several details based on the material examined in our study.

In the daughter rediae of *Neophasis anarrhichae*, the birth canal and birth pore are present but are more distinct in younger specimens (Fig. 7A). Pigmented eyespots are first seen in the cercariae when the tail bud becomes slightly longer than the body (Fig. 7B); they are less prominent than in the cercariae of *N. oculata* (compare Figs. 7D and 3A). An unpigmented eyespot initially emerges as a small dot in the cercarial embryo, staining only with TRITC-labeled phalloidin. We did not trace its further development. The digestive system includes the prepharynx, the pharynx, the oesophagus and the ceca primordia (Fig. 7C). The latter are composed of rows of cells, which do not reach the posterior body end. The cercariae have 13 penetration glands and 11 ducts which are arranged similarly to *N. oculata*. Excretory vesicle is thin-walled, I-shaped or egg-shaped (Fig. 7C and D). Excretory system is of “Mesostoma” type (Fig. 7C). Main collecting ducts divide into anterior and posterior parts near the anterior edge of the ventral sucker (Fig. 7C). Caudal excretory duct is present (Fig. 7C). Mucoïd cytons and mucoïd glands are absent (Fig. 7B, D).

In the metacercariae of *Neophasis anarrhichae* only nine ducts of penetration glands are evident (Fig. 7F). Glandular cells just behind the oral sucker, which were mentioned by Lebour (1910), are in fact a closely packed bunch of ducts. These ducts open at the bottom of the buccal cavity, whereas the glands itself are located laterally to the pharynx. The ceca never reach the posterior body end. Excretory vesicle is egg-shaped (Fig. 7E, I). The metacercariae often retain a short tail, in which the caudal excretory duct is absent. All elements of the reproductive system are clearly distinguishable (Fig. 7E, G, H). There is a lumen in the female and male reproductive ducts (Fig. 7H) and early stages of gametogenesis are commonly observed in the ovary and the testes (Fig. 7G). Formed sperm is found regularly in male gonads. The

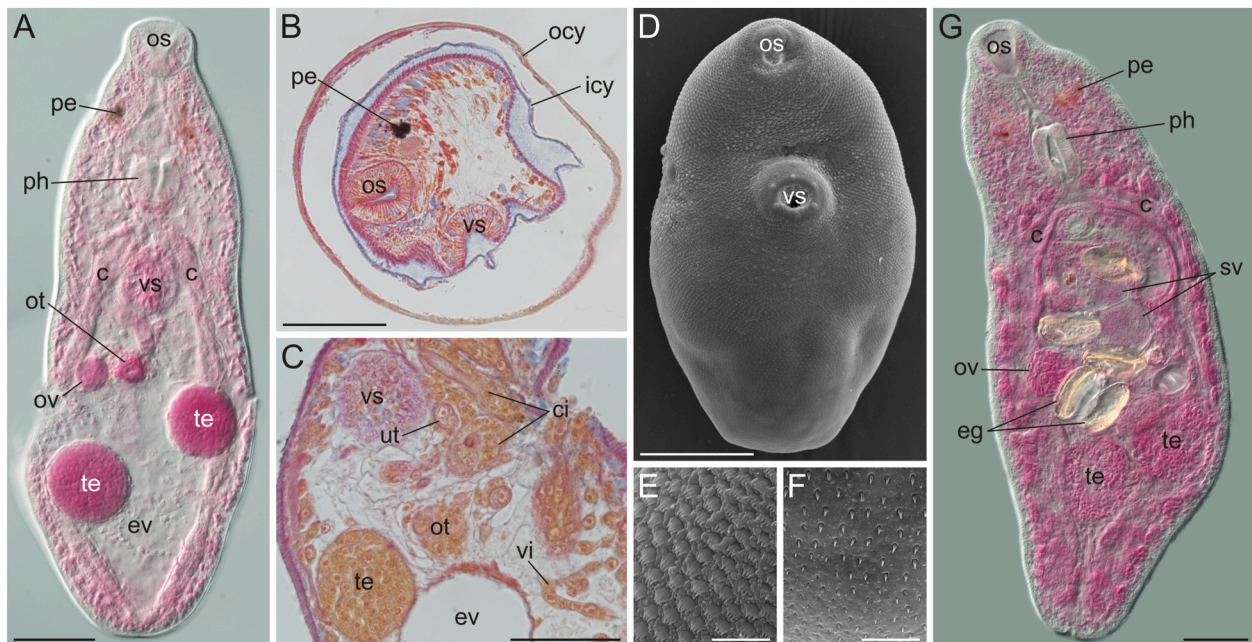


Fig. 5. *Neophasis oculata* metacercariae (A–F) and sexual adult (G). (A) General view of metacercaria (acetic carmine, DIC). (B–C) Histological sections, Mallory's trichrome stain, encysted metacercaria (B) and some of its inner structures (C). (D–F) SEM, ventral view (D) and magnified spines in the anterior (E) and posterior (F) regions. (G) Sexual adult (acetic carmine, DIC). Scale bars – 100 μ m on A, B, D, G; 50 μ m on C; 10 μ m on E, F. Abbreviations: c – ceca; ci – cirrus; eg – eggs; ev – excretory vesicle; icy – inner cyst layer; ocy – outer cyst layer; os – oral sucker; ot – ootype; ov – ovary; pe – pigmented eyespots; ph – pharynx; sv – seminal vesicle; te – testes; ut – uterus; vi – vitelline follicles; vs – ventral sucker.

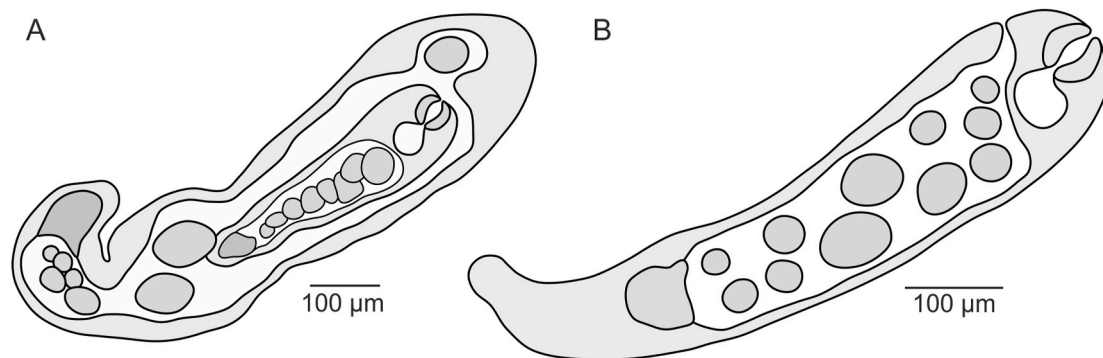


Fig. 6. *Neophasis anarrhichae* mother sporocyst (A) and mother redia (B).

metacercariae can start egg production while they are still within the daughter rediae (Fig. 7I), which was observed in 15 host specimens in 2019–2020.

Remarks: We found a mother sporocyst just once during the observation period. Alongside with it, several mother rediae were present in the kidney of that whelk, while its other organs were free from digenae infection. It seems that the mother rediae are initially located only in the kidney and later move into the digestive and the reproductive gland, where they can be found besides the daughter rediae. The key distinction between them is the content of the brood cavity: mother rediae produce rediae of the next generation whereas daughter rediae produce cercarial embryos.

3.3.5. Sexual adults of *Neophasis anarrhichae* (Fig. 7J)

Locality: White Sea; Keret Archipelago (Kandalaksha Bay).

Host: Atlantic wolffish *Anarrhichas lupus*.

Other reported hosts: *A. denticulatus*, *A. minor* (summarized in Bray and Gibson, 1991).

Site: Intestine.

Prevalence: 77% (17 of 22).

Vouchers: Paragenophores (NA001-NA003) corresponding to isolates No 20 and 21 deposited in the collection of the Department of Invertebrate Zoology of Saint Petersburg University.

Description: Measurements in Table 3.

Remarks: The number of parasites per fish ranged from less than ten to more than 5000 individuals. We found ovigerous sexual adults of *N. anarrhichae* in *A. lupus* throughout the observation period. The most common infection site was the upper midgut. The number of parasites diminished towards the end of the midgut. In heavily infected fish sexual adults were also found in the hindgut, though in lesser numbers than in the midgut. A few immature specimens were sometimes seen in the stomach.

3.4. Phylogenetic position of *Neophasis* spp

Concatenated SSU and LSU dataset comprised 24 sequences and yielded 2977 characters, including gaps. Phylogenetic trees inferred with ML and Bayesian approaches revealed the same topology. The

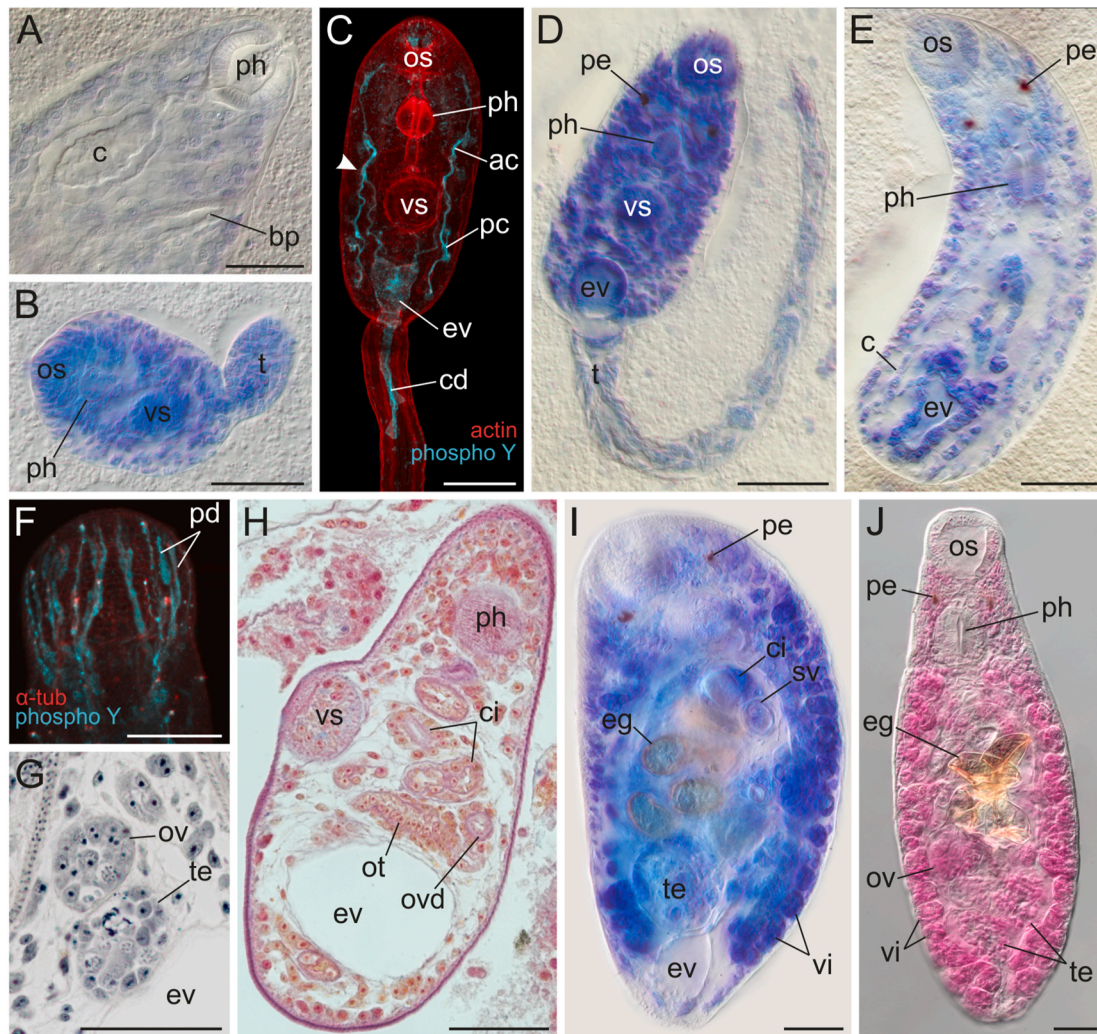


Fig. 7. *Neophasis anarrhichae* successive life cycle stages. (A, B) whole mounts (toluidine blue, DIC) of the anterior end of daughter redia (A) and cercaria embryo (B). (C) Cercaria later embryo, CLSM, TRITC-phalloidin and phospho Y antibody staining. (D, E) whole mounts (toluidine blue, DIC) of cercaria (D) and metacercaria (E). (F) Anterior end of metacercaria with gland ducts, CLSM, acetylated α -tubulin and phospho Y antibody staining. (G) Sagittal section of metacercaria, Heidenhain's iron hematoxylin staining. (H) Sagittal section of metacercaria, Mallory's trichrome stain. (I) progenetic metacercaria (toluidine blue, DIC). (J) sexual adult (acetic carmine, DIC). Scale bars – 50 μ m. Abbreviations: ac – anterior collecting duct; bp – birth pore canal; c – ceca; cd – caudal excretory duct; ci – cirrus; eg – eggs; ev – excretory vesicle; os – oral sucker; ot – ootype; ov – ovary; ovd – oviduct; pc – posterior collecting duct; pe – pigmented eyespots; pd – penetration gland ducts; ph – pharynx; sv – seminal vesicle; t – tail; te – testes; vi – vitelline follicles; vs – ventral sucker. Arrow indicate on site of main collecting duct division. (For interpretation of the references to colour in this figure legend, the reader is referred to the Web version of this article.)

Bayesian tree is presented in Fig. 8; ML bootstrap support values are additionally mapped onto it next to the posterior probabilities (PP) values for all the ML-supported nodes.

There are three well-supported major groups on the tree: Brachycladiidae + Acanthocolpidae clade A and Acanthocolpidae clade B. This is in agreement with previous studies (Bray et al., 2005; Curran and Pulis, 2014; Fraija-Fernández et al., 2015; Kremnev et al., 2020). Two *Neophasis* spp. group together, with high PP and bootstrap support values, within the Acanthocolpidae clade A. This clade also includes *Tormopsolus orientalis* Yamaguti, 1934 and *Pleorchis* spp., but the branching order of these three lineages is unresolved.

4. Discussion

In this study we re-elucidated the three-host life cycle of *Neophasis oculata*, and found that its first intermediate hosts were gastropods *Neptunea despecta* and *Buccinum undatum*. We also verified the two-host life-cycle of *N. anarrhichae*. Genetic differences between the two species of *Neophasis* were shown in ribosomal markers and in mitochondrial COI

gene. We provided the first detailed descriptions of *N. oculata* cercariae and metacercariae, and *N. anarrhichae* mother sporocyst and mother rediae. Previous morphological data on the daughter rediae, cercariae and metacercariae of *N. anarrhichae* were supplemented. The closest relatives of the genus *Neophasis* were shown to be representatives of Acanthocolpidae clade A, genera *Tormopsolus* and *Pleorchis*.

The genus *Neophasis* comprise six species restricted to temperate and cold seas of the Northern Hemisphere (WoRMS, 2021). Only two of them, *N. oculata* and *N. anarrhichae*, have been reported from the North-eastern Atlantic and the adjacent Arctic (Bray and Gibson, 1991). The morphological identification of *N. oculata* from our material is unambiguous, but the specimens of *N. anarrhichae* do not entirely match the morphometric characteristic of this species given by Bray and Gibson (1991), and even resemble another *Neophasis* species, *N. pusilla* Stafford, 1904 (Table 3). However, *N. pusilla* has been recorded only in North-western Atlantic and inhabits not only the intestine but also the urinary and the gall bladder of *Anarrhichas lupus*. Actually, *N. pusilla* and *N. anarrhichae* might be synonymous, as suggested by Bray and Gibson (1991), but this hypothesis has to be checked by molecular methods.

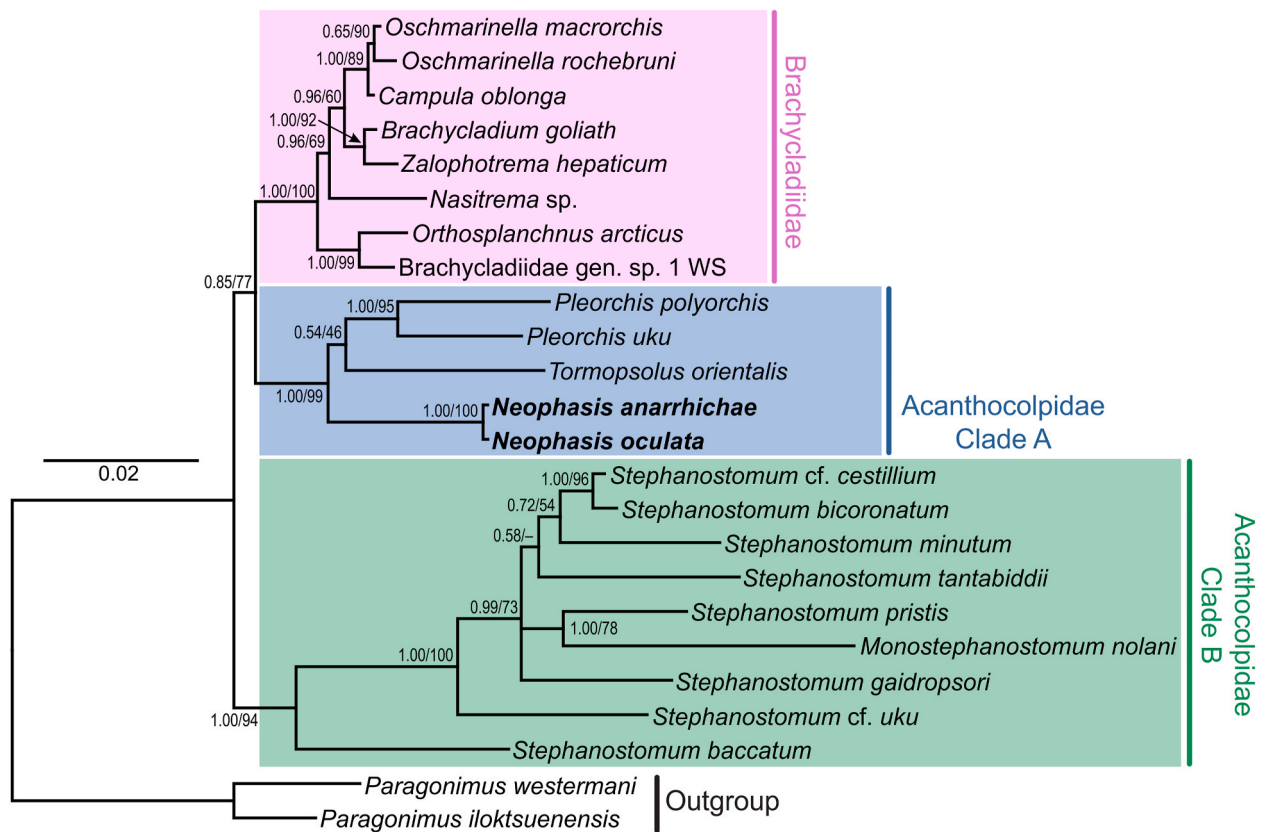


Fig. 8. Phylogenetic position of *Neophasis oculata* and *N. anarrichae* based on the concatenated 18S and 28S rDNA sequence data, inferred with Bayesian inference. Newly generated sequences are indicated in bold. Posterior probabilities are printed at nodes, followed by bootstrap values for the nodes that were also supported in the tree inferred with Maximum likelihood method. Scale bar shows the substitution rate. GenBank accession numbers for the 18S and 28S rDNA sequences are listed in the [Supplementary Table S1](#).

Genetic differences between *N. oculata* and *N. anarrichae* are clearly seen in our data on 18S rDNA (two substitutions), ITS1 (eight substitutions), and 5.8S-ITS2 (one substitution). The D1–D3 domains of 28S rDNA showed no interspecific variation, which is, to our knowledge, the first such case in Digenea. In addition to the sequence divergence, the ITS1 region also includes an unequal number of repeats: seven in *N. anarrichae* and nine in *N. oculata*. As the result, the PCR products differ in length by about 90 b.p. and this molecular “signature” can be detected on the gel prior to sequencing. In general, the genetic distance between *N. oculata* and *N. anarrichae* in the fragments of the ribosomal operon is rather small.

The COI fragments demonstrate a degree of variability consistent with that in other digeneans studied in this respect. The gap between the intra- and interspecific distances is clear and allows an unambiguous delimitation of the boundaries between the two species. The detection of what we consider as numt in *N. anarrichae* is something that the researchers should be aware of when interpreting mitochondrial (mt) DNA sequence data. In contrast to the actual mt COI gene, the numt sequences of *N. anarrichae* lack intraspecific variability. Had this numt not been identified and corrected owing to an alternative primer pair, we could have mistaken it for mt COI, which would have led to erroneous conclusions. This highlights the importance of testing the quality of mt DNA sequence data, e.g. through making sure translated sequences are meaningful and amino acid substitutions are not predicted to have a functional effect on the protein.

The affinity of the genus *Neophasis* to the Acanthocolpidae was predicted by [Bray and Gibson \(1991\)](#) based on the morphology and life cycle data. Here we established the phylogenetic position of this genus by molecular methods for the first time and showed that *Neophasis* spp. formed a branch within the Acanthocolpidae clade A. Based on our and

previous 28S rDNA data, the other members of the clade are *Tormopsolus*, *Pleorchis* and a group of species known only from first intermediate host, *Cercaria capricornia* group 1–3 ([Barnett and Miller, 2018](#); [Kremnev et al., 2020](#)). The latter were uninvolved into our analysis as their 18S rDNA sequences are lacking in GenBank®.

Our molecular data made it possible to verify the life cycle of *N. anarrichae* and to elucidate the life cycle of *N. oculata* ([Fig. 9](#)). The first hypothesis on the life cycle of *N. oculata* was proposed by [Chubrik \(1966\)](#). She found oculate cercariae in the naticid caenogastropod *Cryptonatica affinis* (Gmelin, 1791) and oculate metacercariae in bivalves *Cerastoderma edule* (Linnaeus, 1758) and *Astarte crenata* (Gray, 1824). Based on the superficial morphological similarities shared by the discovered larvae and sexual adults of *N. oculata*, she claimed that three-host life cycle of this species was elucidated. Recently, we have shown that these life cycle stages belong to the family Brachycladiidae ([Kremnev et al., 2020](#)). Here we demonstrate that the first intermediate hosts of *N. oculata* are buccinid gastropods *N. despecta* and *B. undatum* (Neogastropoda: Buccinidae). Cercariae ensure the transmission of infection towards the second intermediate host, *Myoxocephalus scorpius* and other fish species (summarized in [Bray and Gibson, 1991](#)). Encysted metacercariae undergo further development but never reach sexual maturity. Definitive fish hosts (mostly members of the Cottidae—see [Bray and Gibson, 1991](#)) become infected by feeding on the second intermediate hosts. In the White Sea, we found sexual adults of *N. oculata* only in *M. scorpius*, but it was also reported from *M. quadricornis* (Linnaeus, 1758) ([Shulman and Shulman-Albova, 1953](#)). The presence of ovigerous sexual adults mostly in July and infective cercariae mainly in April may indicate the seasonal dynamics in the life cycle.

The only intermediate host of *N. anarrichae* is the common whelk *B. undatum*. The development of all intramolluscan stages was documented

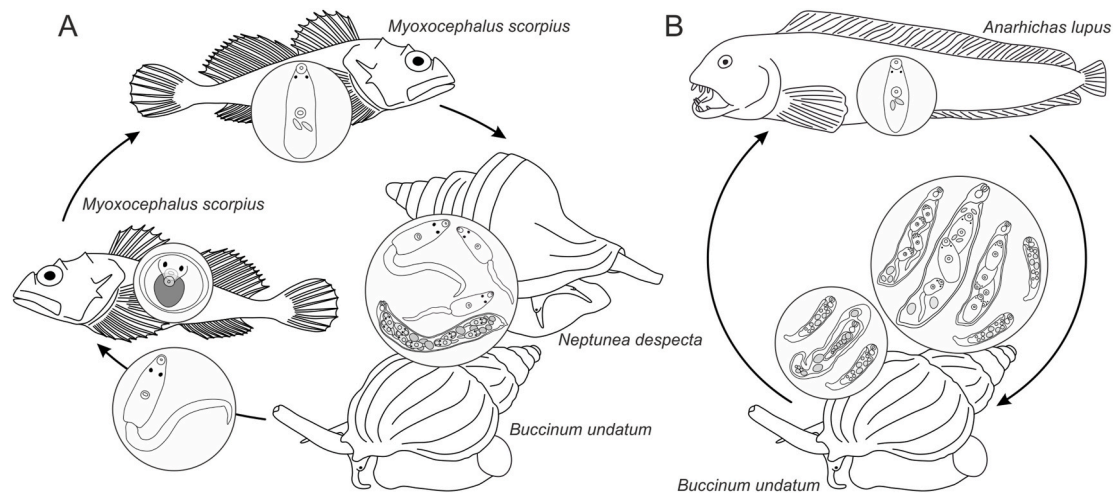


Fig. 9. Proposed life cycle scheme of *Neophasis oculata* (A) and *N. anarrhichae* (B).

in this mollusc. The mother sporocyst was found in the kidney where it produces mother rediae. K  ie (1971) observed a mother sporocyst of *N. anarrhichae* once in a serially sectioned *B. undatum*, but she described it as a small spherical object filled with ~100 rediae and located under the epithelium at the base of the siphon. We think that this mother sporocyst belongs to another digenean species. Mother rediae of *N. anarrhichae* initially accumulate in the kidney but later migrate into the reproductive and the digestive gland, where they begin to produce daughter rediae. As the infection proceeds, daughter rediae can also spread into the kidney, gill, and mantle. Daughter rediae produce cercarial embryos which develop directly into metacercariae without encystment. Metacercariae can achieve sexual maturity and start producing eggs while still within rediae. The definitive host (in the White Sea—only *A. lupus*) becomes infected via ingestion of the whelks with metacercariae.

Early infection stages of *N. oculata* and *N. anarrhichae* in their shared gastropod host, *B. undatum*, may be easily misidentified. To avoid misidentification, one should pay attention to the pigmented eyespots, which are larger in the cercariae of *N. oculata* and appear earlier in the development, and to the mucoid cytons, which are present in *N. oculata* and absent in *N. anarrhichae*. Reexamination of whole mounts stored at the Department of Invertebrate Zoology of Saint Petersburg University (Russia) showed that the cercariae of *N. anarrhichae* described by Chubrik (1966) are actually the underdeveloped cercariae of *N. oculata* from *B. undatum*.

The studied cercariae of *N. oculata* and the cercariae from the closely related Brachycladiidae share several common morphological features: long ceca primordia as rows of cells; presence of three eyespots (two pigmented and one unpigmented); thick-walled I-shaped excretory vesicle; excretory system of the “Mesostoma” type (Kremnev et al., 2020). The cercariae of *N. oculata* and those of brachycladiids can be told apart by the number and arrangement of the penetration glands and the excretory formula, as well as the absence of mucoid glands in the former.

Within the Acanthocolpidae clade A putative cercariae of *Tormosolus* and *Cercaria capricornia* group 1–3 have been described (Bartoli and Gibson, 1998; Barnett et al., 2008). They all have an expanded hindbody, *Cercaria capricornia* group 2 and 3 also possess lateral outgrowths, presumably to attract attention of microphagous fish, which possibly serve as the second intermediate hosts. In contrast, the cercariae of *N. oculata* have a modest appearance, which is probably plesiomorphic for the Acanthocolpidae clade A. Evolutionary changes in the cercarial morphology within the clade may reflect the transition from benthic to planktonic fish as the second intermediate host.

Though the cercariae of *N. anarrhichae* do not leave the molluscan

host, they retain most of the provisional organs such as penetration glands, eyespots, tail. This supports the idea that *N. anarrhichae* evolved from a species with free-swimming cercariae (K  ie, 1973; Bray and Gibson, 1991). However, smaller eyespots and the absence of mucoid cytons in *N. anarrhichae* betrays a loss of adaptations to the transmission of infection from the first to the second intermediate host. Successive development of the digestive and the excretory systems in *N. anarrhichae* and *N. oculata* is also generally similar although ceca in *N. anarrhichae* never reach the posterior region of the body. Nevertheless, unlike *N. oculata*, *N. anarrhichae* continue to grow and mature in the intermediate host: cercariae develop without encystment into metacercariae, infective for the definitive host. The morphogenesis of *N. anarrhichae* may proceed even further: its metacercariae can become sexually mature and start egg production while still in the intermediate host. Thus, its life cycle may become a facultative one-host life cycle, as we described and discussed before (Krupenko et al., 2019).

In our opinion, the transition to continuous morphogenesis of the hermaphroditic generation was crucial for the life cycle truncation within the genus *Neophasis*. In typical three-host digenean life cycles cercariae cannot infect the definitive host, and a second intermediate host is essential for additional morphogenetic changes of the larvae. However, when the cercariae acquire the ability to develop into metacercariae within the mollusc, the second intermediate host becomes superfluous, and its role is taken up by the first intermediate one.

The switch of *N. anarrhichae* to *Anarrhichas* spp. as new definitive hosts was probably due to the diet of these fish, which feed on hard-shelled invertebrates such as molluscs, echinoderms and crustaceans (Bray, 1987; Falk-Petersen et al., 2010). It is noteworthy that only *Buccinum* is the intermediate host of *N. anarrhichae* while another whelk, *Neptunea*, is not. The reason may be associated with a higher accessibility of *Buccinum* to wolffish due to their higher abundance, smaller size and thinner shell.

Secondary dixenous life cycles, with the historical second intermediate host being eliminated and the first intermediate host, the mollusc, taking up its role, are known in eleven digenean families: some species of Microphallidae, Monorchidae, Lissorhiidae, Fellodistomidae, Zogonidae, Gymnophallidae, Gorgoderidae, and all members of Cyclocoelidae, Eucotylidae, Leucochloridiidae and Hasstilesiidae studied in this respect (Bartoli et al., 2000; Poulin and Cribb, 2002; Pina et al., 2009). Secondary dixenous life cycles in the latter four families seem to be associated with life in the terrestrial environment. Evolutionary expansion of the two-host life cycles in the Microphallidae is related to migratory coastal birds in high latitudes (Galaktionov, 2017; Galaktionov and Blasco-Costa, 2018; Galaktionov et al., 2012). *Gymnophallus choledochus* Odhner, 1900 switches from the three-host to the

two-host life cycle in winter (Loos-Frank, 1969). Unlike all these cases, the life cycle truncation in *N. anarrhichae* is apparently not associated with existence under stressful conditions. The seasonal changes are present in the subtidal of the White Sea but are not pronounced in most other parts of *N. anarrhichae* distribution (the North-eastern Atlantic and the southern Barents Sea).

The origin of the two-host life cycle in *N. anarrhichae* seems to have been supported by a strong prey-predator relationship between *A. lupus* and *B. undatum*. Feeding on hard-shelled invertebrates (durophagy) is thought to entail considerable fitness costs, according to the optimal foraging theory (MacArthur and Pianka, 1966; Pyke et al., 1977). Though even non-specialist animals may consume hard-shelled prey under certain conditions (Langerhans et al., 2020), vertebrates generally seem to prefer feeding on arthropods, annelids and other vertebrates rather than gastropods. This may be one of the restrictions standing in the way of life-cycle truncation in digeneans.

Declaration of competing interest

None.

Acknowledgements

This study was supported by the Russian Science Foundation (Russia), grant no. 19-74-10029. The fieldwork was carried out at the Educational and Research Station “Belomorskaia” of Saint Petersburg University (SPbU), Russia, the White Sea Biological Station (WSBS) “Kartesh” of the Zoological Institute of the Russian Academy of Sciences (ZIN RAS), Russia, and the N.A. Pertsov White Sea Biological Station of Moscow State University, Russia. The work at the WSBS “Kartesh” was supported by a research program of ZIN RAS (project no. AAAA-A19-119020690109-2). Our sincere thanks for the help with the sampling are due to Sergei Bagrov, Stanislav Ilyutkin, Olga Knyazeva, Anastasiia Zelenskaia, Olga Skobkina, Arseniy Gubler, Grigoriy Kiselev, Ekaterina Nikitenko, Anna Mikhlin and Irina Ekimova. The authors are particularly grateful to Drs. Anna Romanovich and Aleksey Masharsky for excellent sequencing support. We thank two anonymous reviewers for their helpful comments on the initial version of the manuscript and Natalia Lentsman for linguistic assistance. During research we utilized the equipment of the resource centers “Molecular and Cell Technologies” and “Center for Microscopy and Microanalysis” of the Research park of SPbU and “Taxon” Research Resource Center (<http://www.ckp-rf.ru/ckp/3038/>) of ZIN RAS.

Appendix A. Supplementary data

Supplementary data to this article can be found online at <https://doi.org/10.1016/j.ijppaw.2021.05.001>.

References

- Barnett, L.J., Smales, L.R., Cribb, T.H., 2008. A complex of putative acanthocolpid cercariae (Digenea) from *Nassarius olivaceus* and *N. dorsatus* (Gastropoda: Nassariidae) in central Queensland, Australia. *Zootaxa* 1705 (1), 21–39.
- Barnett, L.J., Miller, T.L., 2018. Phenotypic plasticity of six unusual cercariae in nassariid gastropods and their relationships to the Acanthocolpidae and Brachycladiidae (Digenea). *Parasitol. Int.* 67 (2), 225–232.
- Bartoli, P., Gibson, D.I., 1998. A new acanthocolpid cercaria (Digenea) from *Cantharus dorbignyi* (Prosobranchia) in the western Mediterranean. *Syst. Parasitol.* 40 (3), 175–184.
- Bartoli, P., Jousson, O., Russell-Pinto, F., 2000. The life cycle of *Monorchis parvus* (Digenea: Monorchidae) demonstrated by developmental and molecular data. *J. Parasitol.* 86 (3), 479–489.
- Bowles, J., Hope, M., Tiu, W.U., Liu, X., McManus, D.P., 1993. Nuclear and mitochondrial genetic markers highly conserved between Chinese and Philippine *Schistosoma japonicum*. *Acta Trop.* 55 (4), 217–229.
- Bray, R.A., 1987. A study of the helminth parasites of *Anarhichas lupus* (Perciformes: Anarhichadidae) in the North Atlantic. *J. Fish. Biol.* 31 (2), 237–264.
- Bray, R.A., Gibson, D.I., 1991. The Acanthocolpidae (Digenea) of fishes from the North-east Atlantic: the status of *Neophasis* Stafford, 1904 (Digenea) and a study of north Atlantic forms. *Syst. Parasitol.* 19 (2), 95–117.
- Bray, R.A., Webster, B.L., Bartoli, P., Littlewood, D.T.J., 2005. Relationships within the Acanthocolpidae Lühe, 1906 and their place among the Digenea. *Acta Parasitol.* 50 (4), 281–291.
- Briscoe, A.G., Bray, R.A., Brabec, J., Littlewood, D.T.J., 2016. The mitochondrial genome and ribosomal operon of *Brachycladium goliath* (Digenea: Brachycladiidae) recovered from a stranded minke whale. *Parasitol. Int.* 65 (3), 271–275.
- Choi, Y., Chan, A.P., 2015. PROVEAN web server: a tool to predict the functional effect of amino acid substitutions and indels. *Bioinformatics* 31 (16), 2745–2747.
- Chubrik, G.K., 1966. Fauna and ecology of trematode larvae from molluscs in the Barents and White Seas. *Tr. Murm. Morsk. Biol. Inst.* 10 (14), 78–166 ([in Russian]).
- Curran, S.S., Pulis, E.E., 2014. Confirmation of *Pseudolepidapedon balistis* in the Acanthocolpidae (Digenea) based on phylogenetic analysis of ribosomal DNA. *J. Parasitol.* 100 (6), 856–859.
- Darriba, D., Taboada, G.L., Doallo, R., Posada, D., 2012. jModelTest 2: more models, new heuristics and parallel computing. *Nat. Methods* 9 (8), 772.
- Falk-Petersen, I.B., Kanapathippilai, P., Primicerio, R., Hansen, T.K., 2010. Size, locality and seasonally related feeding preferences of common wolffish (*Anarhichas lupus* L.) from north-Norwegian waters. *Mar. Biol. Res.* 6 (2), 201–212.
- Fraija-Fernández, N., Olson, P.D., Crespo, E.A., Raga, J.A., Aznar, F.J., Fernández, M., 2015. Independent host switching events by digenean parasites of cetaceans inferred from ribosomal DNA. *Int. J. Parasitol.* 45, 167–173.
- Galaktionov, K.V., 2017. Patterns and processes influencing helminth parasites of Arctic coastal communities during climate change. *J. Helminthol.* 91 (4), 387.
- Galaktionov, K.V., Blasco-Costa, I., Olson, P.D., 2012. Life cycles, molecular phylogeny and historical biogeography of the ‘pygmaeus’ microphallids (Digenea: Microphallidae): widespread parasites of marine and coastal birds in the Holarctic. *Parasitology* 139 (10), 1346.
- Galaktionov, K.V., Blasco-Costa, I., 2018. *Microphallus ochotensis* sp. nov. (Digenea, Microphallidae) and relative merits of two-host microphallid life cycles. *Parasitol. Res.* 117 (4), 1051–1068.
- Hernández-Mena, D.I., García-Varela, M., de León, G.P.P., 2017. Filling the gaps in the classification of the Digenea Carus, 1863: systematic position of the Proterodiplostomidae Dubois, 1936 within the superfamily Diplostomoidea Poirier, 1886, inferred from nuclear and mitochondrial DNA sequences. *Syst. Parasitol.* 94 (8), 833–848.
- Koie, M., 1969. On the endoparasites of *Buccinum undatum* L. with special reference to the trematodes. *Ophelia* 6 (1), 251–279.
- Koie, M., 1971. On the histochemistry and ultrastructure of the redia of *Neophasis lageniformis* (Lebour, 1910) (Trematoda, Acanthocolpidae). *Ophelia* 9 (1), 113–143.
- Koie, M., 1973. The host-parasite interface and associated structures of the cercaria and adult *Neophasis lageniformis* (Lebour, 1910). *Ophelia* 12 (1–2), 205–219.
- Kremnev, G., Gonchar, A., Krapivin, V., Knyazeva, O., Krupenko, D., 2020. First elucidation of the life cycle in the family Brachycladiidae (Digenea), parasites of marine mammals. *Int. J. Parasitol.* 50 (12), 997–1009.
- Krupenko, D., Kremnev, G., Krapivin, V., 2019. Possible progenesis in *Neophasis anarrhichae* (Nicoll, 1909) Bray, 1987 in the White Sea. *Parasitol. Int.* 70, 82–85.
- Kumar, S., Stecher, G., Tamura, K., 2016. MEGA7: molecular evolutionary genetics analysis version 7.0 for bigger datasets. *Mol. Biol. Evol.* 33 (7), 1870–1874.
- Lagroe, C., Poulin, R., 2007. Life cycle abbreviation in the trematode *Coitocaeum parvum*: can parasites adjust to variable conditions? *J. Evol. Biol.* 20 (3), 1189–1195.
- Lagroe, C., Poulin, R., 2009. Life cycle abbreviation in trematode parasites and the developmental time hypothesis: is the clock ticking? *J. Evol. Biol.* 22 (8), 1727–1738.
- Langerhans, R.B., Goins, T.R., Stemp, K.M., Riesch, R., Araújo, M.S., Layman, C.A., 2020. Consuming costly prey: optimal foraging and the role of compensatory growth. *Front. Ecol. Evol.* 8, 506.
- Lebour, M.V., 1910. *Acanthopsolus lageniformis*, n. sp., a trematode in the catfish. Northumberland Sea Fisheries Committee. In: Report on the Scientific Investigations for the Year 1909, and to June 15th, 1910, pp. 29–35.
- Lefebvre, F., Poulin, R., 2005. Progenesis in digenean trematodes: a taxonomic and synthetic overview of species reproducing in their second intermediate hosts. *Parasitology* 130 (6), 587.
- Leung, T.L., Donald, K.M., Keeney, D.B., Koehler, A.V., Peoples, R.C., Poulin, R., 2009. Trematode parasites of Otago Harbour (New Zealand) soft-sediment intertidal ecosystems: life cycles, ecological roles and DNA barcodes. *N. Z. J. Mar. Freshw. Res.* 43 (4), 857–865.
- Loos-Frank, B., 1969. Zur Kenntnis der gymnophalliden Trematoden des Nordseeraumes. I. Die Alternativzyklen von *Gymnophallus choledochus* Odhner, 1900. *Z. Parasitenkd.* 32, 135–156 ([in German]).
- Luton, K., Walker, D., Blair, D., 1992. Comparisons of ribosomal internal transcribed spacers from two congeneric species of flukes (Platyhelminthes: Trematoda: Digenea). *Mol. Biochem. Parasitol.* 56 (2), 323–327.
- MacArthur, R.H., Pianka, E.R., 1966. On optimal use of a patchy environment. *Am. Nat.* 100 (916), 603–609.
- Morgan, J.A.T., Blair, D., 1995. Nuclear rDNA ITS sequence variation in the trematode genus *Echinostoma*: an aid to establishing relationships within the 37-collar-spine group. *Parasitology* 111 (5), 609–615.
- Olson, P.D., Cribb, T.H., Tkach, V.V., Bray, R.A., Littlewood, D.T.J., 2003. Phylogeny and classification of the Digenea (Platyhelminthes: Trematoda). *Int. J. Parasitol.* 33 (7), 733–755.
- Pina, S., Tajdari, J., Russell-Pinto, F., Rodrigues, P., 2009. Morphological and molecular studies on life cycle stages of *Diphtherostomum brusinae* (Digenea: Zoogonidae) from northern Portugal. *J. Helminthol.* 83 (4), 321–331.

- Polyansky, Y.I., 1955. Studies on the Parasitology of the Fish in the Northern Seas of the USSR. Parasites of Fish of the Barents Sea, 19, 5–170. Trudy Zoologicheskogo Instituta [In Russian: English translation (1966) Israel Program for Scientific Translations, Cat. No. 1655, 158 pp.].
- Poulin, R., Cribb, T.H., 2002. Trematode life cycles: short is sweet? Trends Parasitol. 18 (4), 176–183.
- Pyke, G.H., Pulliam, H.R., Charnov, E.L., 1977. Optimal foraging: a selective review of theory and tests. Q. Rev. Biol. 52 (2), 137–154.
- Ronquist, F., Teslenko, M., Van Der Mark, P., Ayres, D.L., Darling, A., Höhna, S., Larget, B., Liu, L., Suchard, M.A., Huelsenbeck, J.P., 2012. MrBayes 3.2: efficient Bayesian phylogenetic inference and model choice across a large model space. Syst. Biol. 61 (3), 539–542.
- Schindelin, J., Arganda-Carreras, I., Frise, E., Kaynig, V., Longair, M., Pietzsch, T., Preibisch, S., Rueden, S., Saalfeld, S., Schmid, B., Tinevez, J.Y., White, D.J., Hartenstein, V., Eliceiri, K., Tomancak, P., Cardona, A., 2012. Fiji: an open-source platform for biological-image analysis. Nat. Methods 9, 676–682.
- Shulman, S., Shulman-Albova, R., 1953. Parasites of Fishes of the White Sea. Izdatelstvo Akademia Nauk SSSR, Moskva-Leningrad ([In Russian]).
- Tkach, V., Grabda-Kazubska, B., Pawlowski, J., Swiderski, Z., 1999. Molecular and morphological evidence for close phylogenetic affinities of the genera *Macrodera*, *Leptophallus*, *Metaleptophallus* and *Paralepoderma* [Digenea, Plagiorchiata]. Acta Parasitol. 44 (3), 170–179.
- Villa, M., Lagrue, C., 2019. Progenesis and facultative life cycle abbreviation in trematode parasites: are there more constraints than costs? Int. J. Parasitol. 49 (5), 347–354.
- WoRMS, 2021. *Neophasis* Stafford, 1904. <http://www.marinespecies.org/aphia.php?p=taxdetails&id=108549> on 2021-04-21.

Further reading

- Stamatakis, A., 2014. RAxML version 8: a tool for phylogenetic analysis and post-analysis of large phylogenies. Bioinformatics 30 (9), 1312–1313.